SEISMIC IMAGE ENHANCEMENT BY DOUBLE-WEIGHTED STACKING

PAN DENG[1,2], QIUMING CHENG[3], XIUFA CHEN[4], JIANPING CHEN[3], YU ZHANG[5], FANGYU LI[6] and LEI GUAN[7]

[1] *International Mining Research Center, China Geological Survey, Beijing 100037, P.R. China. dpan@mail.cgs.gov.cn*
[2] *China Mining News, China Geological Survey, Beijing 100037, P.R. China.*
[3] *China University of Geosciences (Beijing), Beijing 100083, P.R. China.*
[4] *Development Research Center, China Geological Survey, Beijing 100037, P.R. China.*
[5] *Wuhan University, Wuhan 430079, P.R. China.*
[6] *Kennesaw State University, Marietta, GA 30060, U.S.A.*
[7] *CNODC, China National Petroleum Corporation (CNPC), Beijing 100034, P.R. China.*

(Received November 7, 2018; revised version accepted September 23, 2020)

ABSTRACT

Deng, P., Cheng, Q., Chen, X., Chen, J.P., Zhang, Y., Li, F.Y. and Guan, L., 2021. Seismic image enhancement by double-weighted stacking. *Journal of Seismic Exploration*, 30: 1-20.

Normal-moveout velocity analysis using semblance spectrum and common-midpoint stacking after normal-moveout correction are two indispensable procedures in seismic reflection data processing, especially for random noise attenuation, velocity model estimation, and imaging quality enhancement. During this process, weighting functions have been frequently used to improve the resolution of semblance and the performance of stacking. In this paper, the interactive relationship between semblance and stacking allows a new method of double-weighted stacking to be created. This method applies the same local-similarity-weighting function to the calculation of both semblance and stacking, aiming to enhance the final stacked image sections. The synthetic and field data numerical experiments have demonstrated that our new approach enhances the signal-to-noise ratio and the reflection-event continuity compared with conventional processing flows.

KEY WORDS: semblance spectrum, normal-moveout correction, double-weighted stacking, local similarity, random noise attenuation, image quality enhancement.

0963-0651/21/$5.00

INTRODUCTION

Stacking technique is quite significant in the tasks of seismic community including preprocessing (Li and Gao, 2014; Chen et al., 2014a,b; Wu et al., 2016; Zhong et al., 2016; Bai and Wu, 2017), Gaussian beam and wave-equation reverse-time migration (Liu et al., 2011; Bai et al., 2016; Ren and Tian, 2016; Chen et al., 2017a,b), full-waveform inversion (Li et al., 2016; Chen et al., 2016), and lithological interpretation (Zhang et al., 2016). It sums the collection of seismic traces with the same midpoint from different shot-receiver pairs, which increases the signal-to-noise ratio (SNR) and the imaging quality of seismic data. Conventional common-midpoint (CMP) stacking is an equal weight or mean stacking that applies the same weighting value on each trace, which is inappropriate for real seismic data because different traces could suffer from different moveout and noise contamination, i.e., nonstationary nature of seismic data. In this case, alternative-weighted stacking methods (Zhang et al., 2004; Neelamani et al., 2006; Trickett, 2007; Liu et al., 2009; Sanchis and Hanssen, 2011; Zhang et al., 2014; Xie et al., 2017; Wu and Bai, 2018a,b) were usually used to overcome the problem of trace difference, in which the different weighting functions for each trace is calculated and applied before stacking.

The inputs for CMP stacking are normal-moveout (NMO) corrected CMP gathers using picked velocities from the semblance spectra. The semblance spectra measure multichannel semblance on the velocity-scanning NMO-corrected gathers; therefore, the accuracy of velocity picking directly influences the CMP-stacking effect. Luo and Hale (2012) introduced a resolution- improved semblance by weighting the data to account for the large-offset data and dampen the small-offset data that increases the resolution of the resulted velocity-scanning map. Chen et al. (2015a) utilized a different weighting strategy for improved velocity spectrum resolution by weighting the data according to the local similarity of each trace with a reference trace within the same CMP gather. Deng et al. (2016) used to a hybrid AB semblance and local similarity strategy to achieve an optimal stacking of the CMP gathers with class II amplitude-variation-with-offset (AVO) polarity-reversal anomaly. AVO-friendly but resolution-loss disadvantage in the AB semblance was dealt with a bootstrapped differential semblance (Wilson and Gross, 2017). Meanwhile, Ebrahimi et al. (2017) used a weighted AB semblance to increase the resolution both in the velocity and time directions.

For improving both the resolution of NMO velocity analysis and the SNR of CMP stacking considering trace difference, we propose to combine local-similarity-weighted semblance and local-similarity-weighted stacking. In this way, the velocity analysis and the subsequent stacking can be an interactive process, because both steps require a good-quality reference trace. More accurate weighted velocity analysis produces flatter NMO-corrected CMP gathers, so that a higher-quality reference trace is provided for

the subsequent weighted stacking. Weighted-stacked trace after CMP stacking then could be used backward as a better reference trace in calculating the weighted semblance for higher resolution in low-SNR data. Therefore, high-resolution velocity analysis and high-quality stacking can contribute positively to each other. Usually three iterations of recursive process are used to obtain the final SNR-allowed and event-continuous stacking sections. Fig. 1 shows the workflow of our proposed double-weighted stacking (DWS) method. The green arrow indicates the recursive process. After the method review, synthetic examples with both high- and low-SNR CMP gathers are tested to demonstrate the performance of our approach. A 2D pre-stack marine dataset from the Gulf of Mexico is also used to implement the workflow of the weighted-velocity analysis and weighted stacking, which demonstrates an obvious improvement compared to the conventional processing flows.

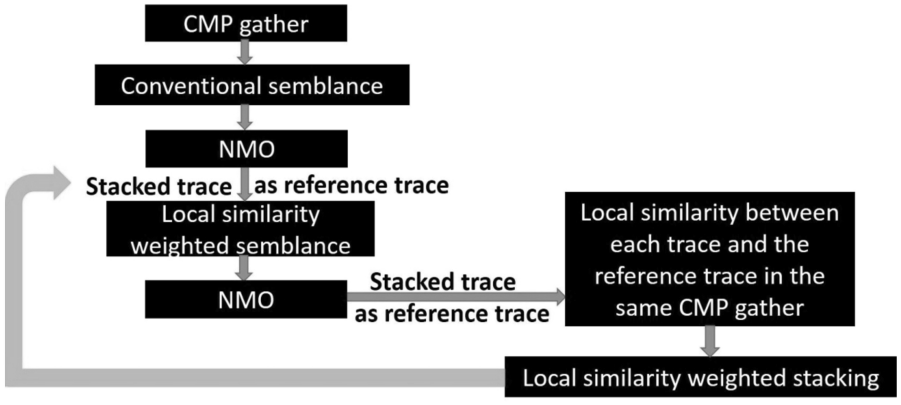

Fig. 1. Workflow of double-weighted stacking.

METHOD

Local similarity

Fomel (2007) defined local similarity of vectors a and b as the square root of element-wise product of c_1 and c_2:

$$c = \sqrt{c_1 * c_2}, \tag{1}$$

where c_1 and c_2 come from two least-squares minimization problems:

$$c_1 = \arg\min_{c_1} \left\| b - Ac_1 \right\|_2^2, \tag{2}$$

$$c_2 = \arg\min_{c_2} \left\| a - Bc_2 \right\|_2^2. \tag{3}$$

where A is a diagonal operator composed from the elements of a: A = *diag*(a) and B is a diagonal operator composed from the elements of b: B = *diag*(b). The least-squares problems (2) and (3) can be solved with the help of shaping regularization (Chen et al., 2015b), which is a smoothness constraint in this case:

$$c_1 = \left[\lambda_1^2 I + T\left(A^T A - \lambda_1^2 I\right)\right]^{-1} T A^T b, \tag{4}$$

$$c_2 = \left[\lambda_2^2 I + T\left(B^T B - \lambda_2^2 I\right)\right]^{-1} T B^T a. \tag{5}$$

where T is a smoothing or shaping operator, and λ_1 and λ_2 are two parameters controlling the physical dimensionality and enabling the fast convergence when inversion is implemented iteratively. These two parameters can be chosen as the L2 norms of A and B, respectively.

We first give a simple synthetic example to illustrate the weighting function by local similarity. Fig. 2 is a 24-fold synthetic CMP gather after NMO correction. There are five traces with erroneous arrivals. They are trace 1 (2 samples earlier), trace 6 (4 samples later), trace 11 (2 samples later), trace 16 (4 samples earlier), and trace 21 (2 samples later).

Fig. 3 shows the local-similarity-weighting function to each trace. They are calculated by the aforementioned calculation method between each trace and a reference trace. A conventional equal-weight or mean stacked trace is chosen as the reference trace here. It is clearly observed that problematic traces are weighted less than the correct traces. Furthermore, different problematic traces have different weighting functions, which are reasonable. More reasonable calculation of weighted semblance and weighted stacking will contribute to a higher resolution of semblance and higher SNR upon stacking; therefore, the principle of local-similarity-weighting is used twice. In the next two subsections, the formulations are given for weighted semblance and weighted stacking by local similarity, respectively.

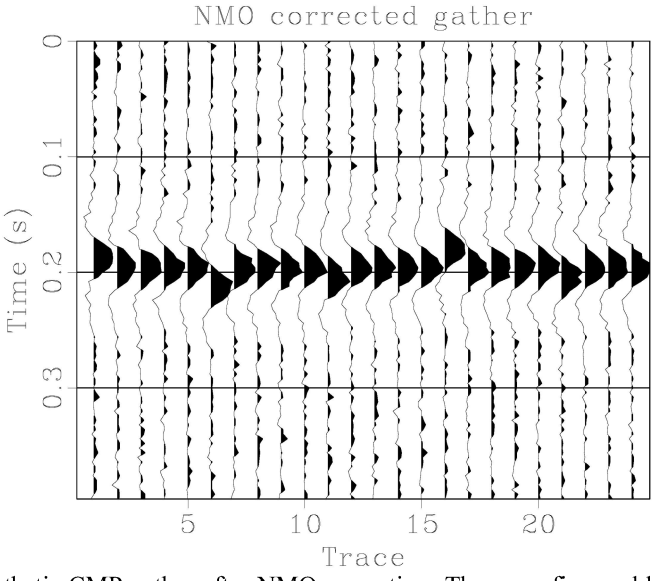

Fig. 2. A synthetic CMP gather after NMO correction. There are five problematic traces inside this gather: trace 1 (2 samples earlier), trace 6 (4 samples later), trace 11 (2 samples later), trace 16 (4 samples earlier), and trace 21 (2 samples later).

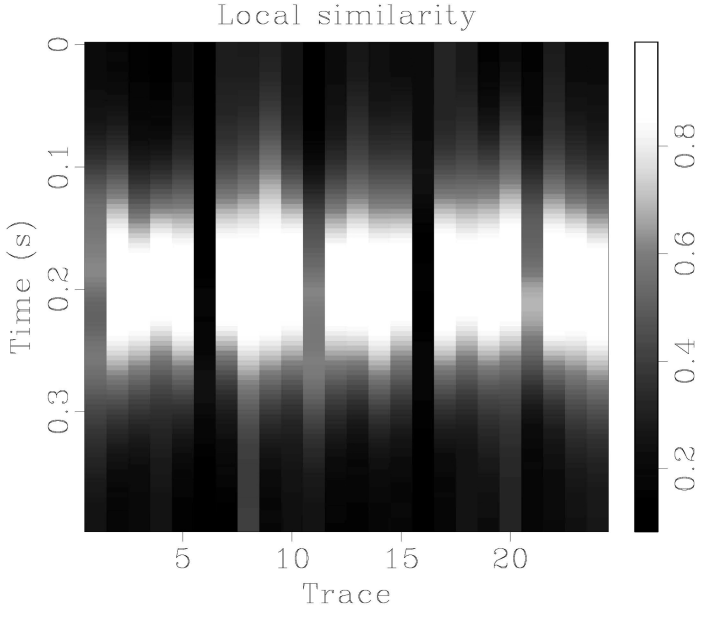

Fig. 3. Local similarity calculated using the CMP gather in Fig. 2 with the conventional stacked trace as a reference trace.

Local-similarity-weighted semblance

The local-similarity-weighted semblance is chosen for NMO velocity analysis in order to improve the resolution of semblance. Conventional semblance can be interpreted as a special case of weighted semblance with the weighting function as a constant, whereas the similarity weighted semblance uses local similarity as the weighting function. More reasonable calculation of local-similarity-weighted semblance is able to produce higher resolution, because the amplitudes with incorrect moveout are suppressed, which reduces the stretch of summation energy in the semblance spectra. The high-resolution semblance could provide accurate NMO velocities for the subsequent NMO correction and stacking. Eqs. (6) and (7) show respectively the calculation of the conventional semblance (Neidell and Taner, 1971) and the weighted semblance.

$$s(k) = \frac{\sum_{i=k-M}^{k+M}\left(\sum_{j=0}^{N-1} d(i,j)\right)^2}{N\sum_{i=k-M}^{k+M}\sum_{j=0}^{N-1} d^2(i,j)}, \tag{6}$$

$$s_w(k) = \frac{\sum_{i=k-M}^{k+M}\left(\sum_{j=0}^{N-1} w(i,j)d(i,j)\right)^2}{\sum_{i=k-M}^{k+M}\left(\sum_{j=0}^{N-1} w^2(i,j)\sum_{j=0}^{N-1} d^2(i,j)\right)}. \tag{7}$$

where $w(i, j)$ is the weighting function, k is the center of the time window, $2M + 1$ is the length of the time window, N is the number of traces in one CMP gather, $d(i, j)$ is the i-th sample amplitude of the j-th trace in the NMO-corrected CMP gather.

Local-similarity-weighted stacking

After the accurate NMO velocities are picked from the high-resolution semblance spectra, local-similarity-weighted stacking scheme is used to stack the flattened NMO-corrected gathers. Eqs. (8) and (9) show the calculation of conventional stacking (Mayne, 1962) and weighted stacking (Liu et al., 2009), respectively.

$$stk(i) = \frac{1}{N}\sum_{j=0}^{N-1} d(i,j), \tag{8}$$

$$stk_w(i) = \frac{1}{\sum_{j=0}^{N-1} w(i,j)}\sum_{j=0}^{N-1} w(i,j)\,d(i,j). \tag{9}$$

where $w(i, j)$ is the weighting function, N is the number of traces in a CMP gather, $d(i, j)$ is the i-th sample amplitude of the j-th trace in the NMO-corrected CMP gather. The local-similarity-weighted stacking is used to substitute the weighting function $w(i, j)$ in eq. (9) with local similarity of each trace and a reference trace in the same CMP gather, where the local similarity should be implemented after the soft thresholding (Donoho, 1995), and the final weighted stacking is averaged by the total number of the non-zero weighted samples in this CMP gather. Usually a conventional equal-weight or mean stacked trace is chosen as the initial reference trace. Flatter CMP gathers using high-resolution weighted semblance in the previous step generate higher-quality reference trace for weighted stacking. In most cases, when the SNR of seismic data is moderate, the choice of a reference trace does not affect the stacked image sections too much. But for low-SNR data, the first weighted-stacked trace after CMP stacking should be used backward as the reference trace for recalculating the higher-resolution weighted semblance. In this case, semblance and stacking become a recursive process, and in common experiments, this iteration will not exceed three times to achieve the final satisfactory stacking results.

EXAMPLES

We apply the proposed method of DWS to two synthetic CMP gathers and a marine dataset. The comparison of semblance spectra, NMO velocities picked, NMO-corrected gathers, and stacked image sections demonstrate the better performance obtained from our approach compared with conventional processing flows.

Synthetic examples

Fig. 4a is the first synthetic CMP gather added with low-level Gaussian white noise (noise variance is 10^{-7}). Figs. 4b and 4c present the comparison of conventional semblance and local-similarity-weighted semblance, where the resolution of the weighted semblance is clearly improved. Fig. 5 is the comparison between NMO-corrected gathers using

different semblance-based velocity analysis. Fig. 6 is the comparison of stacked traces by conventional method in Fig. 6a and DWS in Fig. 6b. It is obvious the new method produces higher SNR than the conventional method.

Fig. 7a is the second synthetic CMP gather added with high-level Gaussian white noise (noise variance is 10^{-6}). Figs. 7b and 7c present the comparison of conventional semblance and local-similarity-weighted semblance. Through a comparison with Fig. 4c and Fig. 7b, Fig. 7c has the highest resolution. It could be concluded that random noise helps focus the energy but may introduce some artifacts beyond the correct picking locations. The problem of these artifacts could be solved with the different parameter settings for local-similarity-weighted semblance and a wiser choice of the reference trace described as the recursive process in the introduction part of this paper. Fig. 8 is the comparison between NMO-corrected gathers using different semblance-based velocity analysis. Fig. 9 is the comparison of stacked traces by conventional method and DWS, which shows the new method in Fig. 9b produces higher SNR than the conventional method in Fig. 9a. The random noise gets well attenuated, especially in the shallow part of the stacked trace in Fig. 9b. Fig. 10 shows the comparison of conventional semblance in Fig. 10a, local-similarity-weighted semblance in Fig. 10b, and recursive-weighted semblance in Fig. 10c. Most artifacts in the conventional semblance and the local-similarity-weighted semblance are removed by the recursive-weighting scheme.

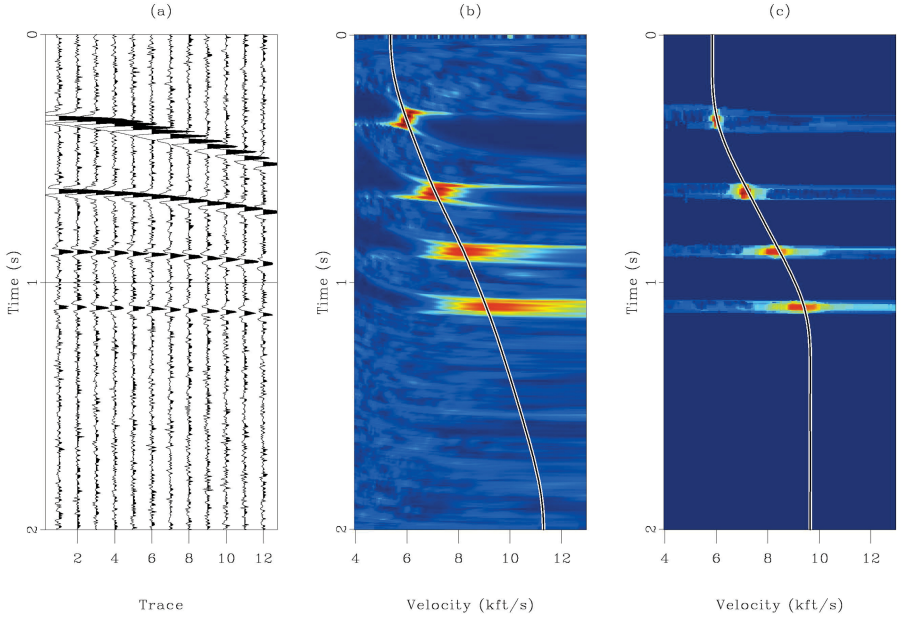

Fig. 4. (a) Synthetic CMP gather added with low-level random noise; (b) Conventional semblance; (c) local-similarity-weighted semblance.

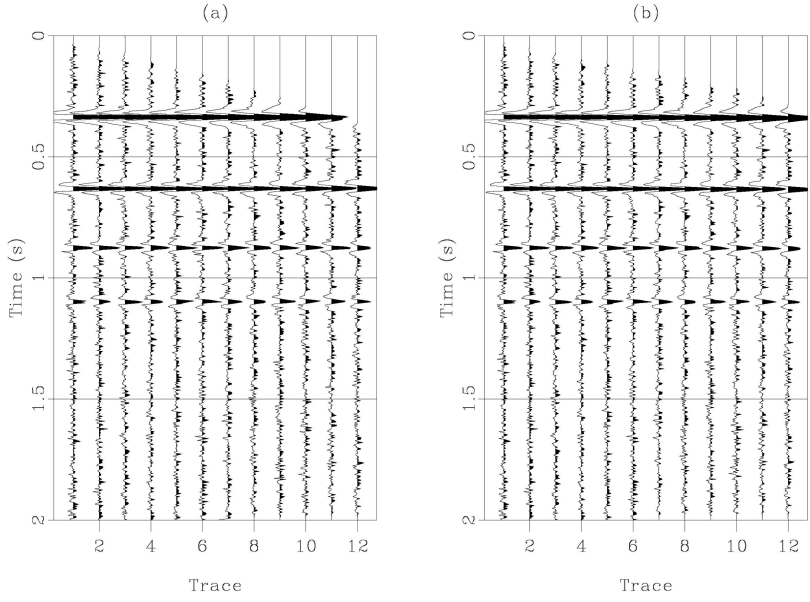

Fig. 5. NMO correction of the CMP gather in Fig. 4a. (a) NMO-corrected gather using the picked velocity from the conventional semblance; (b) NMO-corrected gather using the picked velocity from the local-similarity-weighted semblance.

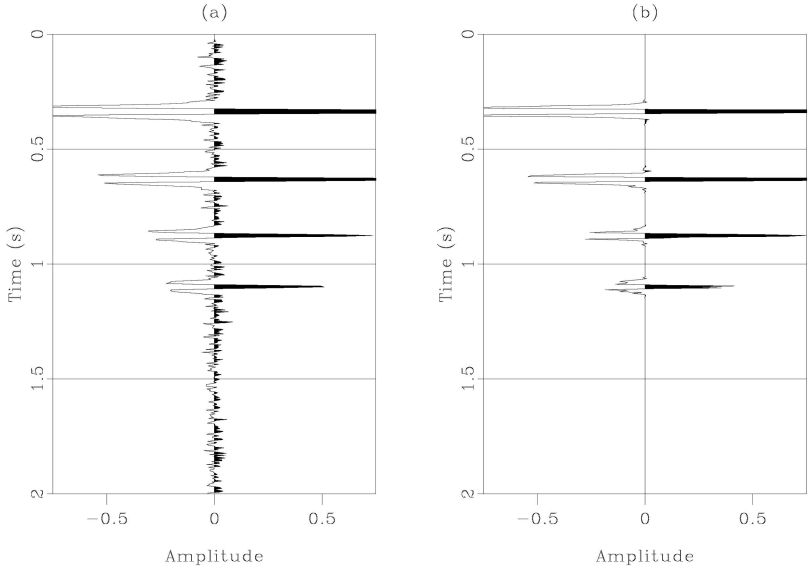

Fig. 6. Stacked trace of the CMP gather in Fig. 4a. (a) Stack by conventional semblance and conventional stacking; (b) Stack by double-weighted stacking.

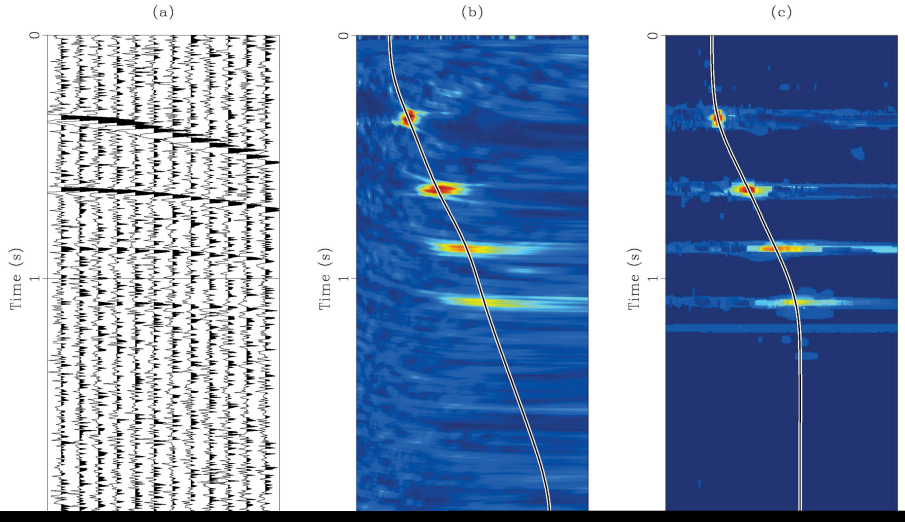
(a)
(b)
(c)
0
1
Time (s)

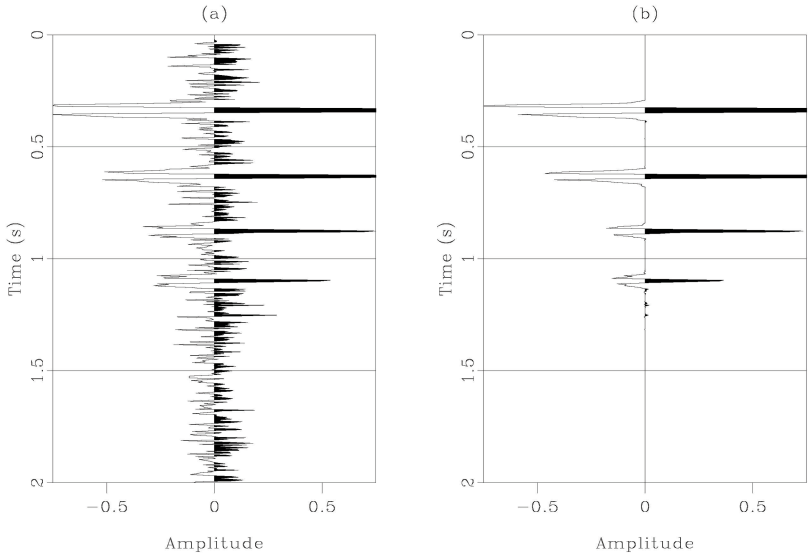

Fig. 9. Stacked trace of the CMP gather in Fig. 7a. (a) Stack by conventional semblance and conventional stacking; (b) Stack by double-weighted stacking.

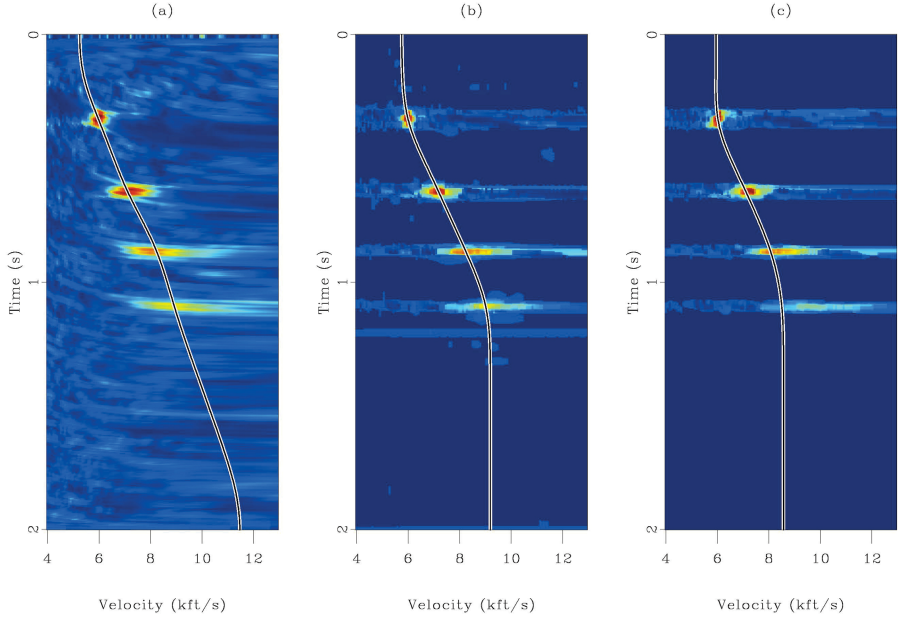

Fig. 10. A comparison of different semblances of the CMP gather in Fig. 7a. (a) Conventional semblance; (b) local-similarity-weighted semblance; (c) Recursive-weighted semblance.

Field examples

A pre-stack field dataset from the Gulf of Mexico (Claerbout, 2005) is used to test our proposed method. Fig. 11 shows the original data in which there is a moderate amount of random noise seen in the reflection events. Fig. 12 is the conventional semblance spectra and Fig. 13 is the local-similarity-weighted semblance spectra. The semblance resolution is enhanced by local similarity weighting. Figs. 14 and 15 show the comparison of different NMO velocities picked from Figs. 12 and 13. Fig. 15 shows a more accurate velocity estimation, especially in the upper right area of the velocity field. Figs. 16 and 17 show the NMO-corrected CMP gathers using the NMO velocities in Figs. 14 and 15. The events in Fig. 17 are flatter resulting from a more accurate velocity estimation. Fig. 18 is the local similarity calculated from the NMO-corrected gathers using local-similarity-weighted semblance-based velocity analysis. The reference trace used here is just the conventional stacked trace. The plot of local similarity is confirmed quite flat, which in turn demonstrates a more accurate NMO velocity analysis by local similarity weighting. The changes of local similarity also match with the properties seen in real data, i.e., larger similarity seen in short-offset and shallow part of the data. Fig. 19 is the stacking section by conventional semblance and conventional stacking. Fig. 20 is the stacked image section by local-similarity-weighted semblance and conventional stacking. Fig. 21 is the stacked image section enhanced by our method that has the higher SNR, signal-energy focus, reflection-event continuity, and structural definition.

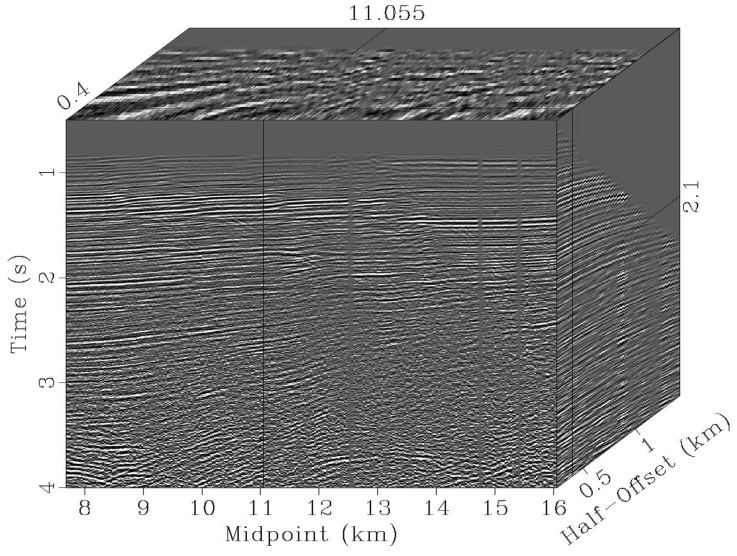

Fig. 11. A pre-stack field dataset from the Gulf of Mexico.

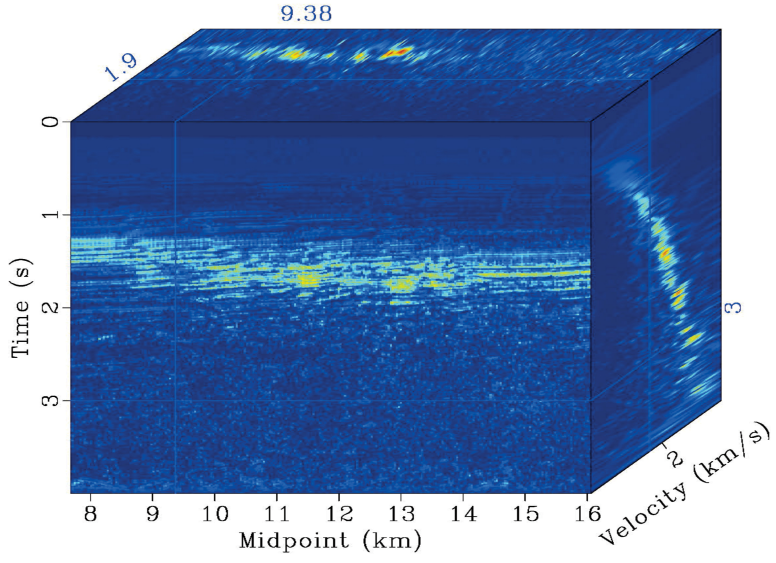

Fig. 12. Conventional semblance spectra.

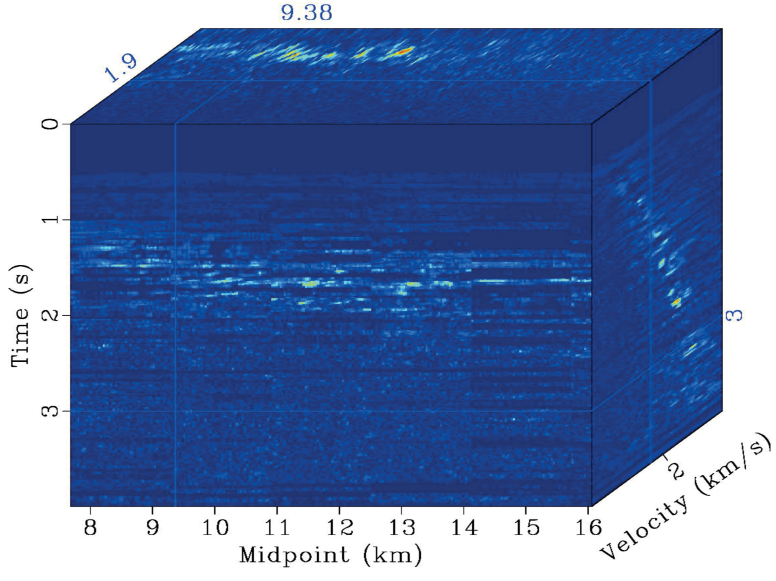

Fig. 13. Local-similarity-weighted semblance spectra.

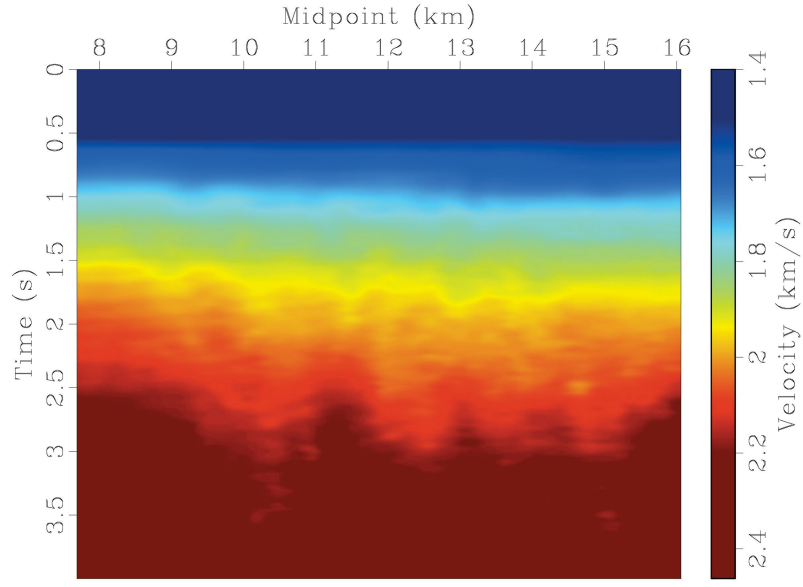

Fig. 14. NMO velocity model picked from the conventional semblance spectra in Fig. 12.

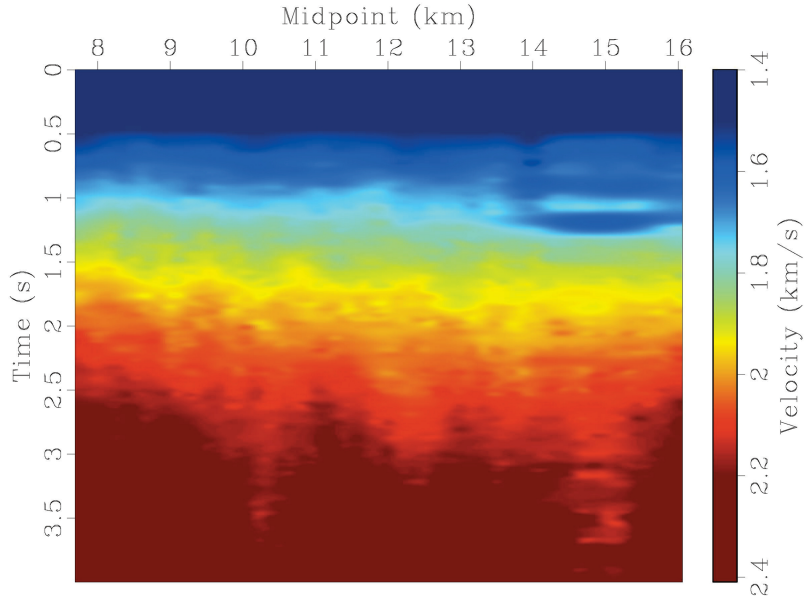

Fig. 15. NMO velocity model picked from the local-similarity-weighted semblance spectra in Fig. 13.

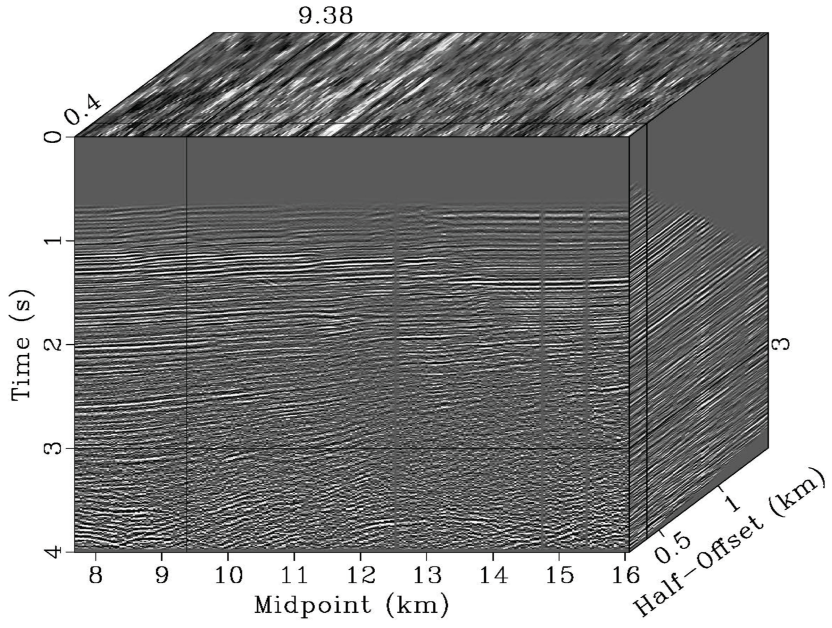

Fig. 16. NMO-corrected CMP gathers using the conventional semblance-based velocity analysis.

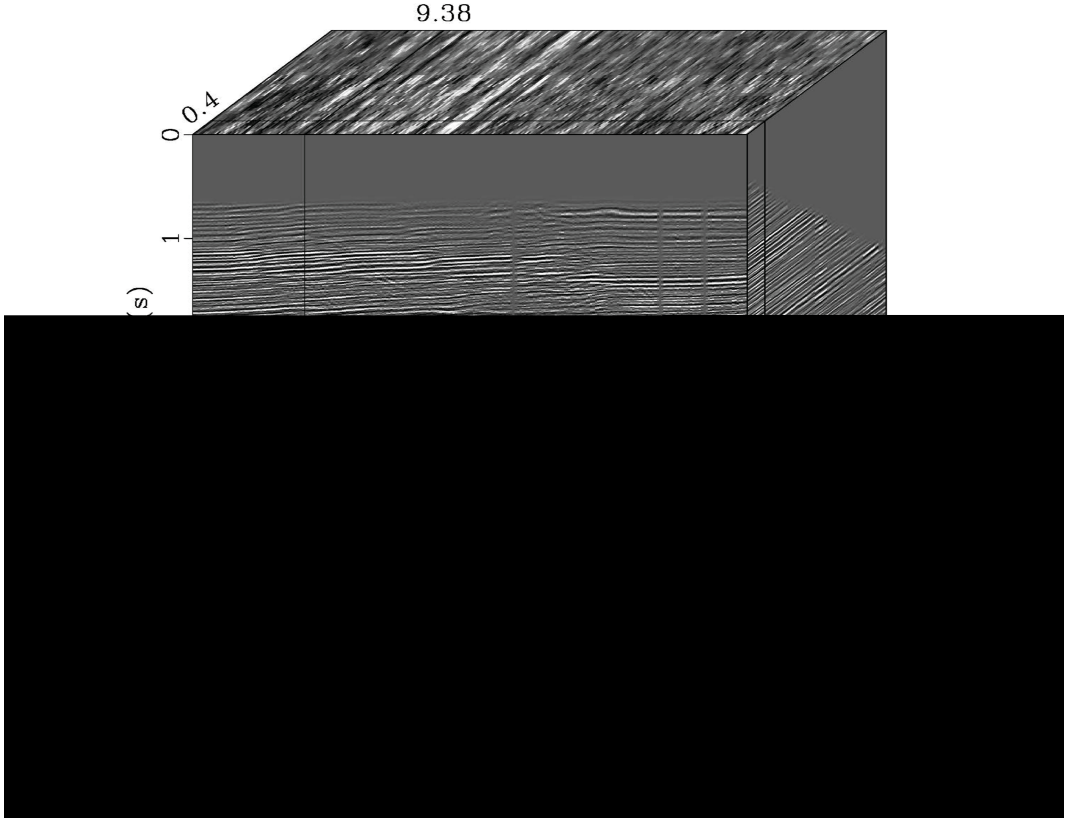

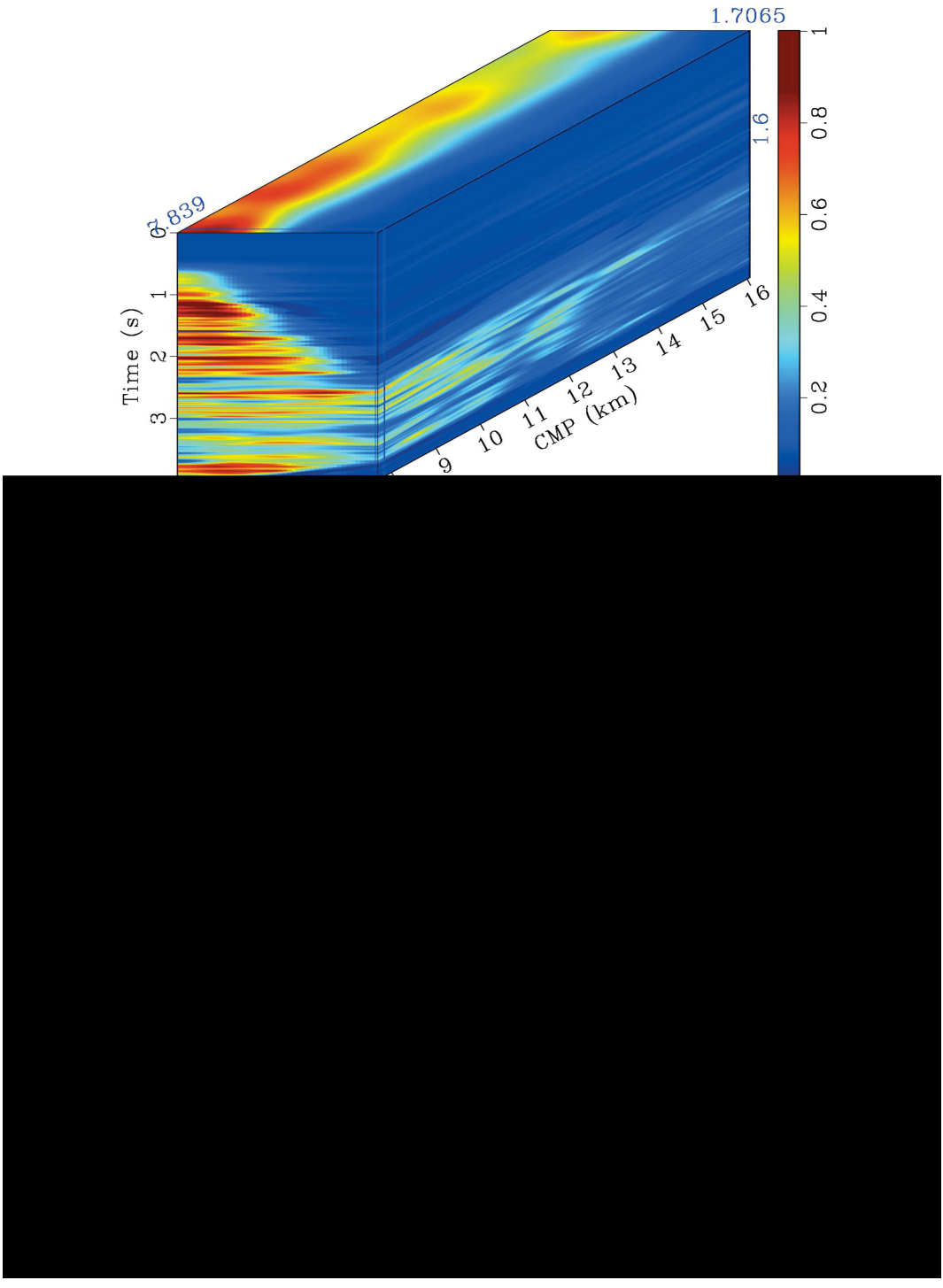
1.7065
1.6
1
0.8
0.6
0.4
0.2
7.839
Time (s)
0
1
2
3
9
10
11
12
13
14
15
16
CMP (km)

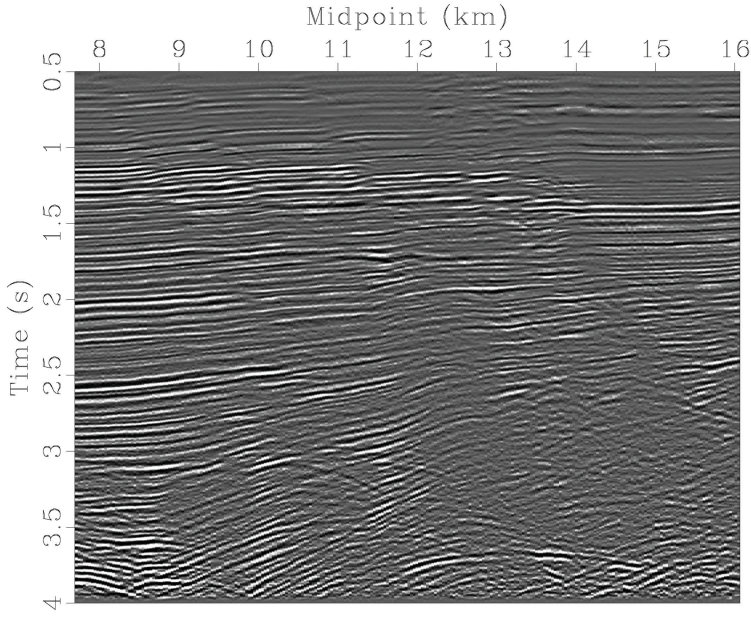

Fig. 20. Stacked image section by local-similarity-weighted semblance and conventional stacking.

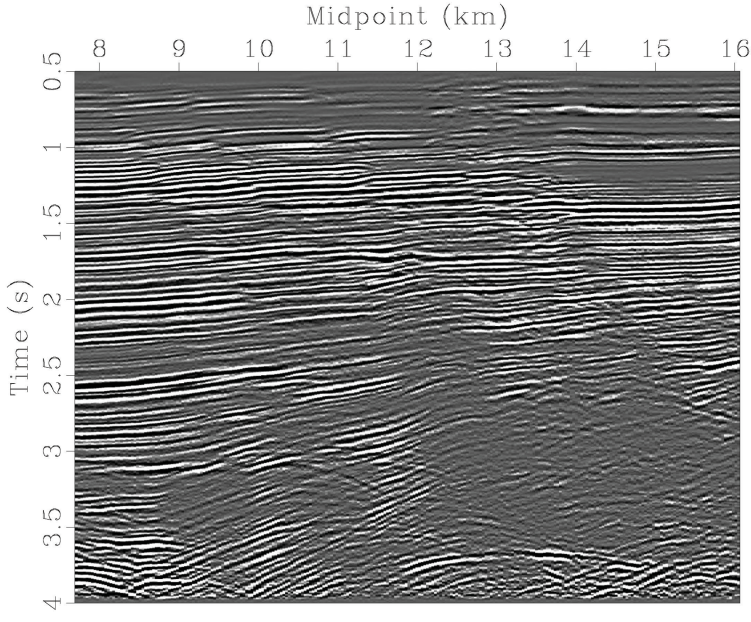

Fig. 21. Double-weighted stacked image section, namely, by local-similarity-weighted semblance and local-similarity-weighted stacking.

DISCUSSION

This study innovates by combining two recent ideas into a complete DWS workflow in seismic reflection data processing, and achieves encouraging results in both synthetic and field testing examples. The proposed method could be applied to most types of seismic reflection data. It can be conveniently implemented based on the framework of conventional semblance calculations and conventional CMP stacking. The key elements in the proposed method are the local-similarity-weighted semblance calculation and local-similarity-weighted stacking, which can be found in the open-source platform, Madagascar; thus, it is worth developing routine processing modules for implementing the proposed workflow.

This method can be applied to data containing sparsely-spaced events in the synthetic data and the closely-spaced events in the field data. Fig. 4c shows an incorrect velocity analysis in the shallow data before the first event. Because of this, local-similarity-weighted semblance may be more appropriate for the analysis of the CMP gathers with closely-spaced reflection events, though the continuity of this semblance seen in Fig. 13 is still waiting to be improved. Meanwhile, through a comparison of Figs. 4c and 7c, the influence of random noise could focus energy but unfortunately introduce artifacts.

Through a comparison of the changes among Figs. 19, 20 and 21, it could be observed that the improvement from Figs. 20 to 21 is larger than that from Figs. 19 to 20. This indicates single weighted-stacking scheme plays a more important role than single weighted-semblance scheme in improving the final stacking effect.

For low-SNR seismic data contaminated by strong noise from subsurface complexity, a recursive process should be used to obtain higher resolution for the recursive-weighted semblance. Higher-resolution recursive-weighted semblance could provide a higher-quality reference trace for weighted stacking, and the entire process leads to an iteration. Although this iteration adds computation cost to the semblance calculations, CMP gather processing can be easily parallelized for efficiency.

CONCLUSIONS

We have proposed a new DWS method that combines local-similarity-weighted semblance and local-similarity-weighted stacking together to improve the performance of final stacking sections. It should be noted that weighted semblance and weighted stacking are not equivalent in improving the final stacking section, and our tests on field data show weighted stacking

plays a larger role. Field data numerical examples demonstrate the effectiveness of the DWS method: high SNR and energy-focused reflection events.

The main drawback of the new workflow lies in the imperfection of the velocity analysis on the CMP gather with sparsely-spaced reflections. Since a reasonable calculation of weighting function depends on the quality of the reference trace, the choice of a more reasonable reference trace and optimal parameter settings should be able to help in solving this problem, and also potentially improving the continuity of the semblance for the data with closely-spaced events.

ACKNOWLEDGMENTS

Pan Deng would like to thank Yangkang Chen at Zhejiang University and Guochang Liu at China University of Petroleum (Beijing) for plentiful and inspiring discussions on similarity-weighted semblance and similarity-weighted stacking. This work was supported by the National Key R&D Program of China (Grant No. 2016YFC0600510 and 2018YFC1505501), the China Geological Survey Project (Grant No. DD20190455, DD20190459, and DD20201181), and the National Natural Science Foundation of China (Grant No. 41872253).

REFERENCES

Bai, M., Chen, X., Wu, J., Liu, G., Chen, Y., Chen, H. and Li, Q., 2016. Q-compensated migration by Gaussian beam summation method. J. Geophys. Engineer., 13: 35-48.

Bai, M. and Wu, J., 2017. Efficient deblending using median filtering without correct normal moveout-with comparison on migrated images. J. Seismic Explor., 26: 455-479.

Chen, Y., Chen, H., Xiang, K. and Chen, X., 2016. Geological structure guided well log interpolation for high-fidelity full waveform inversion. Geophys. J. Internat., 207: 1313-1331.

Chen, G., Fu, L., Chen, K., Sun, W., Wei, W. and Guan, X., 2017a. Calculation of the seismic imaging complexity of complex geological structures. J. Seismic Explor., 26: 81-104.

Chen, Y., Chen, H., Xiang, K. and Chen, X., 2017b. Preserving the discontinuities in least-squares reverse time migration of simultaneous-source data. Geophysics, 82(3): S185-S196.

Chen, Y., Liu, T. and Chen, X., 2015a. Velocity analysis using similarity-weighted semblance. Geophysics, 80(4): A75-A82.

Chen, Y., Liu, T., Chen, X., Li, J. and Wang, E., 2014a. Time-frequency analysis of seismic data using synchrosqueezing wavelet transform. J. Seismic Explor., 23: 303-312.

Chen, Y., Yuan, J., Jin, Z., Chen, K. and Zhang, L., 2014b. Deblending using normal moveout and median filtering in common-midpoint gathers. J. Geophys. Engineer., 11: 045012.

Chen, Y., Zhang, L. and Mo, L., 2015b. Seismic data interpolation using nonlinear shaping regularization. J. Seismic Explor., 24: 327-342.

Claerbout, J.F., 2005. Basic Earth Imaging. Stanford Exploration Project. http://sepwww.stanford.edu/sep/prof/

Deng, P., Chen, Y., Zhang, Y. and Zhou, H., 2016. Weighted stacking of seismic AVO data using hybrid ab semblance and local similarity. J. Geophys. Engineer., 13: 152-163.

Donoho, D.L., 1995. De-noising by soft-thresholding. IEEE Transact. Informat. Theory, 41: 613-627.

Ebrahimi, S., Kahoo, A., Chen, Y. and Porsani, M., 2017. A high-resolution weighted AB semblance for dealing with amplitude-variation-with-offset phenomenon. Geophysics, 82(2): V85-V93.

Fomel, S., 2007. Local seismic attributes. Geophysics, 72(3): A29-A33.

Li, Q. and Gao, J., 2014. Application of seismic data stacking in time-frequency domain. IEEE Geosci. Remote Sens. Lett., 11: 1484-1488.

Li, Y., Li, Z., Zhang, K. and Lin, Y., 2016. Frequency-domain full waveform inversion with rugged free surface based on variable grid finite-difference method. J. Seismic Explor., 25: 543-559.

Liu, G., Fomel, S. and Chen, X., 2011. Stacking angle-domain common-image gathers for normalization of illumination. Geophys. Prosp., 59: 244-255.

Liu, G., Fomel, S., Jin, L. and Chen, X., 2009. Stacking seismic data using local correlation. Geophysics, 74(3): V43-V48.

Luo, S. and Hale, D., 2012. Velocity analysis using weighted semblance. Geophysics, 77(2): U15-U22.

Mayne, W.H., 1962. Common reflection point horizontal data stacking techniques. Geophysics, 27(6): 927-938.

Neelamani, R., Dickens, T.A. and Deffenbaugh, M., 2006. Stack-and-denoise: A new method to stack seismic datasets. Expanded Abstr., 76th Ann. Internat. SEG Mtg., New Orleans: 2827-2831.

Neidell, N.S. and Taner, M.T., 1971. Semblance and other coherency measures for multi-channel data. Geophysics, 36(3): 482-497.

Ren, C. and Tian, X., 2016. Prestack migration based on asymmetric wave-equation extrapolation. J. Seismic Explor., 25: 375-397.

Sanchis, C. and Hanssen, A., 2011. Enhanced local correlation stacking method. Geophysics, 76(3): V33-V45.

Trickett, S., 2007. Maximum-likelihood-estimation stacking. Expanded Abstr., 77th Ann. Internat. SEG Mtg., San Antonio: 2640-2643.

Wilson, H. and Gross, L., 2017. Amplitude variation with offset-friendly bootstrapped differential semblance. Geophysics, 82 (5): V297-V309.

Wu, J. and Bai, M., 2018a. Fast principal component analysis for stacking seismic data. J. Geophys. Engineer., 15: 295-306.

Wu, J. and Bai, M., 2018b. Stacking seismic data based on principal component analysis. J. Seismic Explor., 27: 1-9.

Wu, J., Wang, R., Chen, Y., Zhang, Y., Gan, S. and Zhou, C., 2016. Multiples attenuation using shaping regularization with seislet domain sparsity constraint. J. Seismic Explor., 25: 1-9.

Xie, J., Chen, W., Zhang, D., Zu, S. and Chen, Y., 2017. Application of principal component analysis in weighted stacking of seismic data. IEEE Geosci. Remote Sens. Lett., 14: 1213-1217.

Zhang, G., Tuo, X., Wang, K., Li, B. and Liu, M., 2014. Two-dimensional weighted stack determination using signal-to-noise ratios and probability statistics. Acta Geodaet. Geophys., 49: 431-440.

Zhang, Q., Chen, Y., Guan, H. and Wen, J., 2016. Well-log constrained inversion for lithology characterization: a case study at the jz25-1 oil field, China. J. Seismic Explor., 25:121-139.

Zhang, S., Xu, Y. and Xia, J., 2004. Higher-order correlative stacking for seismic data in the wavelet domain. Expanded Abstr., 74th Ann. Internat. SEG Mtg., Denver: 1433-1436.

Zhong, W., Chen, Y., Gan, S. and Yuan, J., 2016. L1/2 norm regularization for 3D seismic data interpolation. J. Seismic Explor., 25: 257-268.